IEEE Access
Multidisciplinary | Rapid Review | Open Access Journal

Received May 28, 2018, accepted June 23, 2018, date of publication July 2, 2018, date of current version July 25, 2018.

Digital Object Identifier 10.1109/ACCESS.2018.2852067

Global Optimization of All-Optical Hybrid-Casting in Inter-Datacenter Elastic Optical Networks

XIAO LUO[1], CHEN SHI[2], XUE CHEN[1], LIQIAN WANG[1], AND TAO YANG[1]

[1]State Key Laboratory of Information Photonic and Optical Communication, Beijing University of Posts and Telecommunications, Beijing 100876, China
[2]Department of Electrical and Computer Engineering, Iowa State University, Ames, IA 50011, USA

Corresponding author: Xue Chen (xuechen@bupt.edu.cn)

This work was supported by the National Natural Science Foundation of China under Grant 61571061.

ABSTRACT In inter-datacenter elastic optical networks (IDC-EONs), routing, modulation-level, and spectrum assignment (RMLSA) is one of the key measures to increase network capacity and flexibility of spectrum resource management. The coexistence of unicast, anycast, multicast, and manycast traffic in IDC-EONs forms a more complex network communication scheme called hybrid cast. However, the majority of the previous RMLSA approaches focused on the network communication scheme with single traffic type and optimized network performance on the specific network metric, which leads to less practicability and a limit to one-sided network performance improvement. To achieve better network performance, we investigate the hybrid-cast RMLSA (HC-RMLSA) problem with the objective of improving IDC-EON overall performance. Specifically, a criterion is defined to estimate the overall network performance by considering both the overall network service and operation effectiveness and the network cost. An ILP model is formulated to solve the HC-RMLSA problem under static network scenario. Then, we propose an independent optimization genetic algorithm with priority-based rationality adaption (IOGA-PRA) by coordinating a set of hybrid-cast requests simultaneously to solve the HC-RMLSA problem under both static and dynamic network scenarios. Numerical results show that the performance of IOGA-PRA is very close to the optimal solutions obtained by the ILP model on the network cost-effectiveness in static network scenario. The IOGA-PRA also achieves outstanding improvement of the overall network performance compared with benchmark algorithms in the dynamic network scenario.

INDEX TERMS Elastic optical networks (EONs), global optimization, hybrid-cast, inter-datacenter, routing, modulation level, and spectrum assignment (RMLSA).

I. INTRODUCTION

With the emerging data-intensive applications (e.g., Google App Engine, IBM Blue Cloud, social networking), which produce huge amounts of data, optical interconnected datacenters (DCs) are worldwide deployed in cloud infrastructures for data processing and storage. For instance, Google has to refresh its indexes by crawling over 20 billion websites every day, so that it can ensure the results returned to users' queries are as current as possible. All these computational-intensive tasks are done in warehouse-scale computers (WSCs), which are commonly known as mega DCs in Google's optical inter-DC networks [1]. Generally, DCs are interconnected to form geographically distributed datacenter networks (DCNs) which provide massive information technology (IT) resources, i.e., computational, memory and storage resources.

There are two main traffic types in inter-DCNs, user-to-DC traffic and DC-to-DC traffic [2]. The former is related to user-driven communication, which aims to request services and access resources in DCs. The latter mainly processes the demands among DCs, e.g., content backup, synchronization, replication and updating. User-to-DC traffic is typically loaded by unicast and anycast [3] communication schemes, which are point-to-point (PTP) transmission where the destination of anycast is selected from multiple candidate DCs with the same services. Multicast [4] and manycast [5], the point-to-multipoint (PTM) communication schemes, are applied to DC-to-DC traffic for efficient transmission of huge bandwidth capacity, where destinations of manycast are determined from a set of candidate DCs. By contrast to multicast, the high flexibility in destination nodes selection of manycast makes it appropriate in huge

data transmission, such as DC distributed backup, cloud/grid computing. The coexistence of above four types of requests, denoted as hybrid-cast, completely covers the basic traffic types of inter-DCNs [6]. With the rapid growth of diversity and flexibility of applications in IDC-EONs, the hybrid-cast will become a promising communication scheme for efficient and comprehensive supporting such heterogeneous service transmission.

To meet the increasing capacity requirements, optical network provides interconnected DCs a viable and reliable infrastructure to support high-throughput traffic. In addition, with technologies of optical orthogonal frequency division multiplexing (O-OFDM) and Nyquist wavelength division multiplexing (NWDM) enabled, elastic optical networks (EONs) [7], [8] have emerged which support much finer spectrum granularity allocation (e.g., 6.25GHz or 12.5GHz) and superchannel transmission at 400 Gbit/s and beyond as well. EONs that provide enhanced spectral efficiency and more flexible spectrum allocation in optical layer, become a promising candidate for future optical DCNs. Thus, the inter-DCNs have been changed to flexible and heterogeneous in terms of bit rate, center frequency spacing, modulation format and optical reach, when underlying infrastructure is inter-DC EONs (IDC-EONs) [9]. Basically, to address the efficient network resource utilization among DCs, one of the main problems is the routing, modulation level, and spectrum assignment (RMLSA) in IDC-EONs [10]. A number of studies investigate RMLSA problem with different objectives measured by one or more network metrics, e.g., network capacity, network quality of service (QoS) and network energy consumption (NEC) [11]–[13]. Nevertheless, the improvement of a particular network metric may find it difficult to adapt overall IDC-EON demands [14]. In addition, there are interacted effects and restrictions among network metrics, which makes the improvement of network performance more complex according to one or more particular network metrics. Commonly, we pay attention to optimize the request blocking probability (RBP), e.g., to increase the number of served requests, which leads to the NEC increasing in IDC-EONs on the other hand. It is hard to measure the network performance only depending on the gains of RBP, because there is the increasing expense of NEC. Thus, it is necessary to enable global optimization of overall network performance in IDC-EONs by coordinating the main network performance metrics to reach a better match between network operation and user demands. Although the improvement of particular network metric in global optimization may be worse than that in the corresponding exclusive optimization, the balance among main metrics is improved and the global improvement of network performance, i.e., the improvement of all involved network metrics, is reached.

In this paper, we investigate the global optimization of IDC-EONs that supports hybrid-cast communication scheme. With generalizing the expression of hybrid-cast requests, the hybrid-cast RMLSA (HC-RMLSA) problem is solved by involving the interacted effects of main network metrics to network performance. Our contributions consist of three aspects.

1) To measure overall network performance efficiently, we define a network performance criterion to consider the trade-off among main network metrics, i.e., the number of served and blocked requests, the actual type of request, network throughput, transmission distance and NEC.
2) An ILP model is formulated to solve HC-RMLSA problem with the objective of improving overall network performance. It jointly conducts routing lightpath/light-tree construction, modulation level assignment, and spectrum resource allocation.
3) An independent optimization genetic algorithm (GA) with priority based rationality adaption (IOGA-PRA) is proposed to address the HC-RMLSA problem in both static IDC-EON planning and dynamic IDC-EON provisioning. Request priority principle and spectrum conflict (SC) link priority principle are defined to order the incoming request and fiber links in network. IOGA-PRA processes a set of ordered hybrid-cast requests (HCRs) simultaneously by coordinating the rationality of non-fixed HC-RMLSA solutions of them.

The rest of the paper is organized as follows. Section II summarizes the related work. Section III introduces the network model and overall network performance evaluation criterion. Section IV formulates the ILP model for HC-RMLSA problem. We describe the proposed heuristic in Section V. Section VI gives numerical simulation results. Finally, in Section VII, we conclude this paper.

II. RELATED WORKS

Different communication schemes in optical DCNs have been well studied, in which the routing and wavelength assignment (RWA) problems with different optimization objectives have attracted much attention [15]–[17]. The survivable anycasting was considered in [15]. Authors addressed content placement, routing, and protection of paths and content together. An integrated ILP, two-step ILP, linear program relaxation of the two-step ILP and heuristics were proposed to solve the problem of content placement with content protection and routing with path protection. Muhammad *et al.* [16] investigated the RWA problem for inter-DC content replication with manycast and anycast traffic synchronously. The literature aims to reduce the overall network capacity usage by proposing an ILP model and an efficient heuristic with significant network capacity reduction. The static network scenarios with unicast and multicast traffic were investigated in [17], authors developed an ILP model and a light-tree based heuristic to minimize the network resource consumption. However, there is nearly no literature investigating the hybrid-cast communication scheme and the global optimization of network to the best of our knowledge.

With the emergence of EON, the number of literatures about IDC-EON with different communication schemes and objectives increases rapidly [5], [18]–[20].

Fallahpour *et al.* [5] studied energy efficient manycast RMLSA problem and proposed two heuristics by considering two types of DCs. Although the heuristics made obvious improvements in both energy saving and RBP reduction by selecting the most energy efficient manycast light-tree from all available candidates, the collaboration of these two metrics with other important network metrics, such as network cost and transmission reach, has not been involved. The unicast and anycast traffic were considered in [18], and authors proposed heuristics to address available RMLSA by involving the extra regenerators to approach the trade-off between RBP and network cost. Nevertheless, the static RMLSA with unicast and anycast traffic has not been mentioned. The routing and spectrum assignment (RSA) problem for anycast requests was addressed in [19]. Several heuristics were proposed by considering the computing and bandwidth resources jointly for efficient service provisioning. To enhance the DC service resilience responsiveness, a novel global resources integrated resilience (GRIR) algorithm was proposed in [20]. However, improving the resilience of network is the main objective of GRIR without considering other network performance metrics.

Moreover, there are some literatures about solving RSA/RMLSA problem by leveraging GA framework [21]–[23], due to its powerful solution searching ability and algorithm scalability. Owing to the differences in application communication scheme, i.e., hybrid-casting, and optimization objective, i.e., the evaluation and improvement of overall network performance, our work is fundamentally different from the existing GA-based works.

III. NETWORK ARCHITECTURE WITH HYBRID-CAST TRAFFICS

A. INTER-DATACENTER NETWORK MODEL

We consider a directed graph $G(V, E)$ to represent the IDC-EON's physical topology, where V and E denote the set of nodes and fiber links, respectively. Fig.1 illustrates a simple IDC-EON network architecture with main network elements. Concretely, all nodes in V are equipped with bandwidth-variable optical transponders (BV-OPTs) and splitter and delivery switch based multicast optical cross connects (MC-OXCs) [24]. In this paper, the MC-OXC processes PTP and PTM requests separately to avoid extra optical power reduction of PTP requests. The PTM request crosses through splitter to optical switch while PTP request goes to switch directly, shown in Fig. 1. We assume that there is no limitation on the number of output optical channels in MC-OXC. The architecture can simply be an optical splitter replicating the input signal to output ports followed by utilizing optical amplifier (OA) to compensate the power loss.

B. HYBRID-CAST COMMUNICATION SCHEME

We define the generalized expression of HCRs as $HR_i = \{s_i, D_i, k_i, C_i\}$, where i is the request ID and s_i denotes source node. $D_i = \{d_1, d_2, \ldots, d_j\}$ is a candidate destination node set, in which d_j is the jth candidate destination. k_i is the number of destinations that should be connected and C_i is request capacity. When $|D_i| = k_i = 1$, the actual type of HCR is unicast; when $|D_i| > k_i = 1$, the actual type of HCR is anycast, when $|D_i| = k_i > 1$, the actual type of HCR is multicast, and when $|D_i| > k_i > 1$, the actual type of HCR is manycast. As traffic types in network change with time variation, the proportion of requests with different actual types in hybrid-cast communication scheme should be changed correspondingly. Since the user-to-DC traffic and DC-to-DC traffic are concentrated on daytime and night time respectively [25], we consider three traffic models in IDC-EON, i.e., the proportion of HCRs with PTP and PTM transmission (PPM) are 2:1, 1:2 and 1:1, to cover the typical hybrid-cast communication schemes.

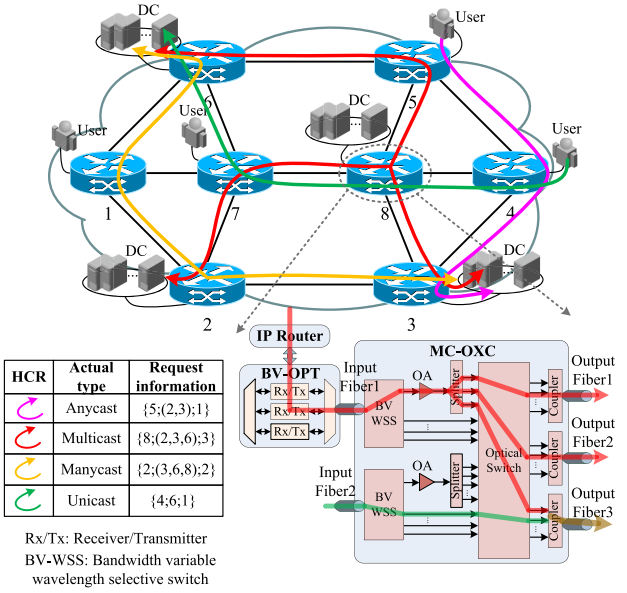

FIGURE 1. An example of hybrid-cast scenario under six-node IDC-EON architecture.

1) HYBRID-CAST ROUTING

The HCR is routed in two different ways according to its actual request type. We assume that light-path and light-tree are applied to serve the HCRs with the corresponding PTP and PTM transmissions. The light-tree is the combination of light-paths from source to each destination [26]. In Fig. 1, the routing light-paths and light-trees of four HCRs with different actual types are illustrated, in which the destinations of HCRs with actual type of manycast and anycast are randomly determined. Since we consider all-optical hybrid-casting without spectrum conversions, the modulation format and assigned FS's stay unchanged for all links on a light-path and light-tree.

2) MODULATION LEVEL ASSIGNMENT

In this paper, the modulation formats that can be used for data transmission are binary phase-shifted keying (BPSK),

quadrature phase-shifted keying (QPSK), eight-quadrature amplitude modulation (8-QAM) and 16-QAM, according to receiver sensitivities [27]. The detailed mapping relationship between modulation formats and maximum transmission reaches is referred to [24] which are restricted by fiber nonlinearity impairments. We assume that the highest modulation level has always been selected among the available candidate modulation formats for the highest spectral efficiency.

3) SPECTRUM RESOURCE ALLOCATION

We assume that each fiber link $e \in E$ has a total bandwidth capacity of F FS's, and each FS occupies a fixed capacity of C_{BPSK} Gbit/s when modulation format is BPSK. m is defined as the modulation level, where $m = 1, 2, 3, 4$ for BPSK, QPSK, 8-QAM, and 16-QAM, respectively. Hence, the capacity of a FS under different modulation formats is represented as $m \cdot C_{BPSK}$ Gbit/s. The number of assigned contiguous FS's for each HCR, denoted as n_i, can be calculated as follows.

$$n_i = \left\lceil \frac{C_i}{m_i \cdot C_{BPSK}} \right\rceil + g_b \tag{1}$$

where m_i is the assigned modulation level of ith HCR and g_b represents the number of FS's used for guard-band defined as 1 in this paper.

C. OVERALL NETWORK PERFORMANCE FORMULATION

To evaluate the overall network performance with hybrid-cast traffic, we define a new criterion, the cost-effectiveness value σ, shown as follows.

$$\sigma = \frac{SOE_{ptp} + SOE_{ptm}}{\cos t_{ptp} + \cos t_{ptm}} \tag{2}$$

In (2), SOE_{ptp} is the network service and operation effectiveness (SOE) affected by HCRs with PTP transmission while SOE_{ptm} is the SOE affected by HCRs with PTM transmission. $cost_{ptp}$ and $cost_{ptm}$ are the network cost of serving HCRs with transmission of PTP and PTM, respectively. A HCR is treated as the smallest granularity and the overall network performance is translated as the accumulation of the impact of each HCR to network performance. It is worth mentioning that σ can be used to evaluate network performance in both static and dynamic network scenarios because it measures network performance after network complete change without considering intermediate process. The detailed explanations of (2) are summarized as follows.

1) THE SOE PART OF (2)

As the development trend of the optical network, the higher the capacity per fiber, the higher the capacity per optical channel and the longer transmission distance is [7], which demonstrates that network capacity and transmission reach are the two main factors to measure network effectiveness [28]. Thus, the larger capacity and longer transmission reach, the better its network effectiveness in IDC-EON is. We fully define network SOE in (3) and (4).

$$SOE_{ptp} = \left|I_s^{ptp}\right| \cdot \sum_{i \in I_s^{ptp}} (C_i \cdot lp_i) - \left|I_b^{ptp}\right| \cdot \sum_{i \in I_b^{ptp}} (C_i \cdot lp_i), i \in I^{ptp} \tag{3}$$

$$SOE_{ptm} = \left|I_s^{ptm}\right| \cdot \sum_{i \in I_s^{ptm}} (C_i \cdot lt_i) - \left|I_b^{ptm}\right| \cdot \sum_{i \in I_b^{ptm}} (C_i \cdot lt_i), i \in I^{ptm} \tag{4}$$

In (3) and (4), I^{ptp} and I^{ptm} are the set of HCRs with PTP and PTM transmission, respectively. I_s^{ptp} is the set of successful served HCRs with PTP transmission while I_s^{ptm} is that with PTM transmission. I_b^{ptp} and I_b^{ptm} are the respective set of blocked HCRs with transmission of PTP and PTM. lp_i is the length of the shortest light-path of the ith HCR and lt_i is the sum of all the shortest light-paths' length of the ith HCR which is from source to each destination. The network SOE is measured as the accumulated effect of each HCR to network capacity and reach. As the product of network capacity and transmission reach can be used as a measure to estimate the effectiveness of network [29], $C_i \cdot lp_i$ and $C_i \cdot lt_i$ are used to measure the network effectiveness affected by HCRs with PTP and PTM transmission accordingly. Note that lp_i and lt_i are not the length of actual routing light-path and light-tree of the ith HCR. The effect of a HCR to network transmission reach should be considered as an available distance from source to destination when there are multiple routing paths that can be selected. Essentially, the available distance from source to destination is the shortest light-path for well-planned network topology since the physical distance of the network has already been fixed. Moreover, the effect of a HCR to network effectiveness is regarded as either positive or negative, which corresponds to be served or blocked. Thus, the numbers of served and blocked HCRs are used to reflect the degree of the effect of HCRs to network effectiveness. This is because the more HCRs served successfully, the better service performance of the network is, and it can further increase the actual network capacity.

2) THE COST PART OF (2)

Network cost for installing and operating optical network can be generally divided into capital expenditure (CapEx) and operational expenditure (OpEx) [30]. CapEx consists of the cost for purchasing network components and initial installing and deploying of network infrastructures. OpEx, on the other hand, refers to the cost of operating and maintaining network, e.g., personal cost and power cost. The optical network is typically designed to minimize its CapEx by coordinating appropriate static RSA/RMLSA schemes at the network plan and deployment stage [31], while the CapEx of network changes slightly at normal network operation stage without considering network disaster and update. In this paper, we mainly evaluate the network performance during

operation stage, in which the minimum CapEx of network has already been achieved in the network setting up stage and it stays almost constant during network operating stage. Hence, we assume that CapEx can be ignored in this paper due to its slight influence in the total network cost. In OpEx, NEC has become a key parameter due to the increasing network capacity which consumes non-negligible amount of energy [32]. Furthermore, comparing to other network operation and maintaining cost in OpEx, the variation of power cost is closely related to network planning and provisioning when the network infrastructures are determined. Thus, OpEx is simplified as NEC for total network cost in this paper. Equations (5) and (6) show the corresponding network cost calculation of HCRs with PTP and PTM transmission.

$$\cos t_{ptp} = \sum_{i \in I_s^{ptp}} PC_{lp_i^{al}} \tag{5}$$

$$\cos t_{ptm} = \sum_{i \in I_s^{ptm}} PC_{lt_i^{al}} \tag{6}$$

In (5) and (6), $PC_{lp_i^{al}}$ is the sum of energy consumption of nodes and links in actual routing light-path of the ith HCR with PTP transmission, while $PC_{lt_i^{al}}$ is the sum of energy consumption of all branches in actual routing light-tree of the ith HCR with PTM transmission. In this paper, we consider the same power model proposed in [5] by involving traffic dependent and traffic independent network elements. The energy consumption value of each element is also acquired from [5]. In IDC-EONs, IP router and BV-OPT are the main power consumption elements in source. The MC-OXC (that is, bandwidth-variable OXC, BV-OXC) and OA are the major power consumption elements in intermediate elastic-bandwidth router and transmission fiber link accordingly. Hence, the energy consumption of served HCRs with transmission of PTP and PTM are correspondingly demonstrated as follows.

$$\begin{aligned} PC_{lp_i^{al}} = {} & \delta_{ip}^{s_i} \cdot pc_{ip}^{idp} + pc_{ip}^{dp} \cdot tr_i + \delta_{bvt}^{s_i} \cdot pc_{bvt}^{idp} + pc_{bvt}^{dp} \cdot tr_i \\ & + \delta_{ip}^{d_{ij}} \cdot pc_{ip}^{idp} + pc_{ip}^{dp} \cdot tr_i + \delta_{bvt}^{d_{ij}} \cdot pc_{bvt}^{idp} + pc_{bvt}^{dp} \cdot tr_i \\ & + \sum_q \left(\delta_{oxc}^k \cdot pc_{oxc}^{idp} \right) + \sum_g \left(\delta_{oa}^{(m,n)} \cdot pc_{oa} \right) \end{aligned} \tag{7}$$

$$\begin{aligned} PC_{lt_i^{al}} = {} & \delta_{ip}^{s_i} \cdot pc_{ip}^{idp} + pc_{ip}^{dp} \cdot tr_i + \delta_{bvt}^{s_i} \cdot pc_{bvt}^{idp} + pc_{bvt}^{dp} \cdot tr_i \\ & + \sum_{j=1}^{|D_i|} \begin{pmatrix} \delta_{ip}^{d_{ij}} \cdot pc_{ip}^{idp} + pc_{ip}^{dp} \cdot tr_i + \delta_{bvt}^{d_{ij}} \cdot pc_{bvt}^{idp} \\ + pc_{bvt}^{dp} \cdot tr_i \end{pmatrix} \\ & + \sum_q \left(\delta_{oxc}^k \cdot pc_{oxc}^{idp} \right) + \sum_g \left(\delta_{oa}^{(m,n)} \cdot pc_{oa} \right) \end{aligned} \tag{8}$$

In (7) and (8), pc_{ip}^{idp}, pc_{bvt}^{idp} and pc_{oxc}^{idp} are the traffic independent power consumption of IP router, BV-OPT and BV-OXC, respectively. pc_{ip}^{dp} and pc_{bvt}^{dp} are the respective traffic dependent power consumption of IP router and BV-OPT. pc_{oa} is power consumption of a OA. Moreover, δ_{ip}^k, δ_{bvt}^k, δ_{oxc}^k and $\delta_{oa}^{(m,n)}$ are binary variables indicating respective state of IP router, BV-OPT and BV-OXC in node k and OA in fiber link e_{mn}, where active state equals to 0 and idle state equals to 1.tr_i denotes traffic load in Gbit/s. Coefficient q and g are the respective number of intermediate nodes and OAs in fiber links of the actual routing light-path and light-tree.

IV. ILP FORMULATION

In this section, the proposed ILP formulation is described. We consider each HCR as an information flow which goes through links from source to each determined destination. According to the actual type of HCR, the optimal light-path is constructed for HCR with PTP transmission and light-tree for HCR with PTM transmission. At the same time, the corresponding modulation level is selected adaptively by transmission distance and contiguous FS's are assigned.

Notation:

$G(V, E)$: Physical network topology.

V: Network node set.

E: Network link set, $e_{mn} \in E$ when there is a physical fiber link between node m and n.

I: HCR set, $i \in I$.

s_i: The source node of the ith HCR.

D_i: The candidate destination node set of the ith HCR.

k_i: The number of destination nodes should be connected of the ith HCR.

C_i: The requested capacity of the ith HCR.

len_{mn}: The length of link $e_{mn} \in E$.

Len_h: The maximum transmission length under modulation level h.

ML: Modulation level set contains four available modulation levels, i.e., modulation level equals 1 for BPSK, 2 for QPSK, 3 for 8-QAM and 4 for 16-QAM.

Variables:

m_i: An integer variable that represents the modulation level of the ith HCR.

n_i: An integer variable that represents the number of contiguous FS's assigned to the ith HCR.

v_i: An integer variable that represents the first FS index of the ith HCR.

w_i: An integer variable that represents the last FS index of the ith HCR.

z_{mn}^i : An integer variable that represents the number of times the link $e_{nm} \in E$ used by the ith HCR.

M_{m_i} : A binary variable, which is equal to 1 if and only if the modulation level of the ith HCR is m_i.

H_n^i : A binary variable, which is equal to 1 if and only if $n \in V$ belongs to the ith HCR.

l_{nm}^i : A binary variable, which is equal to 1 if and only if link $e_{nm} \in E$ has been used for the ith HCR.

$f_{nm}^{i,d_{ij}}$: A binary variable which is equal to 1 if and only if there is a flow on link $e_{nm} \in E$ that heads to the destination $d_{ij} \in D_i$.

$x_{i,t}$: A binary variable, which is equal to 1 if and only if the ith HCR and the tth HCR has common link(s).

$y_{i,t}$: A binary variable, which is equal to 1 if and only if the first FS index of the ith HCR is smaller than the first FS index of the tth HCR.

Objective:

$$\text{Maximize } \sigma = \frac{SOE_{ptp} + SOE_{ptm}}{\cos t_{ptp} + \cos t_{ptm}} \tag{9}$$

The optimization objective is to maximize the cost-effectiveness of network to reach the better overall network performance.

Constraints:

Light-path/light-tree construction constraints:

$$H^i_{s_i} = 1, \quad \forall i \in I \tag{10}$$

$$\sum_{j=0}^{|D_i|} H^i_{d_{ij}} = k_i, \quad \forall i \in I \tag{11}$$

$$\sum_{m \in V} l^i_{ms_i} = 0, \forall i \in I \tag{12}$$

$$\sum_{m \in V} l^i_{mn} = H^i_n, \forall i \in I, n \neq s_i \tag{13}$$

$$\sum_{m \in V} l^i_{nm} \geq H^i_n, \forall i \in I, \forall n \notin D_i \tag{14}$$

Equations (10) and (11) add the corresponding source and destination(s) for each HCR. Equation (12) ensures the basic structure of light-path/light-tree. Equation (13) ensures that the nodes except source have an incoming fiber link in light-path/light-tree. In addition, (14) ensures that the intermediate nodes in light-path/light-tree have at least one outgoing fiber link.

Light-path/light-tree flow constraints:

$$\sum_{m \in V} f^{i,d_{ij}}_{md_{ij}} = 1, \quad \forall i \in I, d_{ij} \in D_i \tag{15}$$

$$\sum_{m \in V} f^{i,d_{ij}}_{d_{ij}m} = 0, \quad \forall i \in I, d_{ij} \in D_i \tag{16}$$

$$\sum_{d_{ij} \in D_i} \sum_{m \in V} f^{i,d_{ij}}_{ms_i} = 0, \quad \forall i \in I \tag{17}$$

$$\sum_{m \in V} f^{i,d_{ij}}_{s_i m} = 1, \quad \forall i \in I, d_{ij} \in D_i \tag{18}$$

$$\sum_{m \in V} f^{i,d_{ij}}_{mn} = \sum_{m \in V} f^{i,d_{ij}}_{nm}, \quad \forall i \in I, d_{ij} \in D_i, n \notin \{s_i, d_{ij}\} \tag{19}$$

$$l^i_{mn} \leq \sum_{d_{ij} \in D_i} f^{i,d_{ij}}_{mn}, \quad \forall i \in I \tag{20}$$

$$\sum_{d_{ij} \in D_i} f^{i,d_{ij}}_{mn} \leq |V| \cdot l^i_{mn}, \forall i \in I \tag{21}$$

Equations (15) and (16) ensure that there should be an incoming flow and no outgoing flow in each destination. Equations (17) and (18) guarantee that there is no incoming flow to source node and there are exact numbers of outgoing flows to each destination. Equation (19) ensures that there is the same numbers of incoming and outgoing flows in each intermediate node. Equations (20) and (21) warrant that each fiber link should hold at least one flow and the total number of flows on each link should not exceed the number of destinations.

Modulation level selection constraints:

$$\sum_{m_i \in ML} M_{m_i} = 1, \quad \forall i \in I \tag{22}$$

$$\sum_{d_{ij} \in D_i} f^{i,d_{ij}}_{mn} \cdot len_{mn} \leq Len_{m_i} \cdot M_{m_i}, \quad \forall i \in I \tag{23}$$

Equation (22) ensures that only one modulation level is selected to each HCR, while Equation (23) ensures that the selected modulation can guarantee the longest transmission distance of light-tree/light-tree of each HCR.

Spectrum assignment constraints:

$$n_i \geq \left\lceil \frac{C_i}{m_i \cdot C_{BPSK}} \right\rceil + g_b, \quad \forall i \in I \tag{24}$$

$$x_{i,t} \geq z^i_{mn} + z^t_{mn} - 1, \forall i, t \in I, e_{mn} \in E \tag{25}$$

$$y_{i,t} + y_{t,i} = 1, \quad \forall i, t \in I \tag{26}$$

$$w_t - v_i + 1 \leq F \cdot \left(1 + y_{i,t} - x_{i,t}\right), \quad \forall i, t \in I, i \neq t \tag{27}$$

$$w_i - v_t + 1 \leq F \cdot \left(2 - y_{i,t} - x_{i,t}\right), \quad \forall i, t \in I, i \neq t \tag{28}$$

$$w_i - v_i + 1 \geq n_i, \forall i \in I \tag{29}$$

Equation (24) determines the number of FS's to be assigned to each HCR. Equation (25) ensures that all common links between two HCRs are handled. Equations (26)-(28) ensure that no spectrum overlap on the common link(s) is used by two different HCRs. Equation (29) ensures that the assigned contiguous FS's of each HCR satisfy its capacity.

V. HEURISTIC ALGORITHM

The mathematical formulation of the HC-RMLSA problem with the improvement of overall network performance presented in Section IV can be used to find the optimal solution in principle. However, high computational complexity makes ILP model not suitable for solving large-scale HC-RMLSA problem. In this section, we propose a time-efficient GA based heuristic, which focuses on processing a set of HCRs at a time to increase the cooperation of them to approach global optimization of network performance.

A. INDEPENDENT OPTIMIZATION GENETIC ALGORITHM

GA framework is an optimization strategy with strong searching ability that mimics the natural evolution [33]. To describe the principles of planning a set of HCRs under GA framework with request-independent optimization in detail, Fig. 2(a) shows the correspondence between elements in HC-RMLSA problem and proposed independent optimization genetic algorithm (IOGA). The smallest granularity in IOGA is a gene, which stands for an available HC-RMLSA solution of a HCR in request set in HC-RMLSA problem. A set of genes constitute a chromosome, which stands for an available HC-RMLSA scheme of a set of HCRs. Here we only list 12 genes in a chromosome as an example in Fig. 2 (a), while the number of genes in a chromosome depends on the request set. A population, which consists by a set of chromosomes,

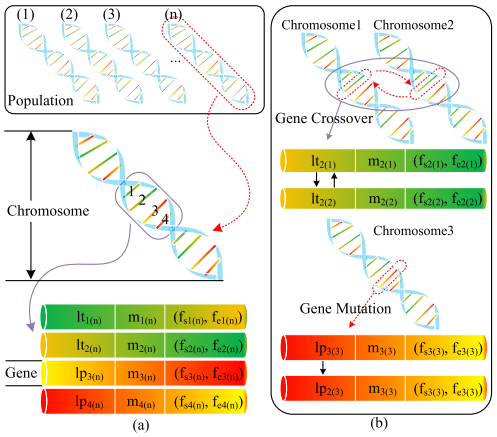

FIGURE 2. (a) Relationship among gene, chromosome and population in IOGA, (b) detailed operations of gene crossover and mutation.

stands for various candidate HC-RMLSA schemes for the set of HCRs. Concretely, we define a population as P, the ath chromosome in P as Ch^a, the ith gene in Ch^a as g_i^a. A gene is detailed encoded as $g_i^a = \{lp_{i(a)}/lt_{i(a)}, m_{i(a)}, (f_{si(a)}, f_{ei(a)})\}$, shown in Algorithm 1, lines 4-12, where $lp_{i(a)}/lt_{i(a)}$ denotes the ath possible routing light-path or light-tree for the ith HCR, i.e., when the HCR is served with PTP transmission, $lp_{i(a)}$ is applied, otherwise $lt_{i(a)}$ is applied. The destination node(s) is randomly selected from the candidate destination node set to form a light-path or light-tree when the actual type of HCR is anycast or manycast. $m_{i(a)}$ is the corresponding modulation level for the ith HCR based on $lp_{i(a)}/lt_{i(a)}$, and $(f_{si(a)}, f_{ei(a)})$ are the allocated start and end FS index of the ith HCR in the ath chromosome. Note that the FS allocation here is request-independent and allocated FS's are non-fixed, which means the FS allocation of all HCRs in the same request set (chromosome) that only depends on the fixed spectrum occupation of current network state. This request-independent FS allocation may cause SC among genes, i.e., the same FS's are allocated to multiple genes. In chromosome generation phase, gene encoding procedures are repeated for all HCRs in request set I, and a chromosome that contains $|I|$ genes can be constructed. Then, we change different routing light-paths/light-trees in some or all genes to form new chromosomes until P is complete. It is worth mentioning that Gong *et al.* [23] have proposed an efficient GA based heuristic in EONs with multicast traffic. Nevertheless, it encoded each multicast request as multiple separated unicast requests whereas our proposed IOGA encodes each HCR directly by its actual type without request decomposition. Furthermore, the algorithm proposed in [23] is applied to process single request at a time while the IOGA is adopted to solve the request-independent HC-RMLSA scheme of a set of HCRs.

Under GA framework, the population is evolved in generations and there are four basic operations in every iteration that are shown in Algorithm 1, lines 16-20, i.e., fitness value calculation, chromosome selection, gene crossover and gene mutation. The fitness value is a criterion that can be used to estimate evolution of IOGA. We set the objective of

Algorithm 1 IOGA

Input: $G(V, E)$, a HCR set I.
Output: HC-RMLSA scheme with non-fixed SC, Q_{sc}.
1 $Q_{sc} \leftarrow \emptyset$, $P \leftarrow \emptyset$;
2 **while** $|P|$ is less than threshold **do**
3 $Ch^a \leftarrow \emptyset$;
4 **for** request $i \in I$ **do**
5 identify actual type of HCR;
6 select candidate $lp_{i(a)}/lt_{i(a)}$ randomly;
7 assign $m_{i(a)}$ based on $lp_{i(a)}/lt_{i(a)}$;
8 calculate $n_{i(a)}$ based on $m_{i(a)}$ and C_i;
9 allocate request-independent contiguous $(f_{si(a)}, f_{ei(a)})$ by *First_Fit Algorithm*;
10 construct a gene as $g_i^a = \{lp_{i(a)}/lt_{i(a)}, m_{i(a)}, (f_{si(a)}, f_{ei(a)})\}$;
11 insert g_i^a into Ch^a;
12 **end for**
13 insert Ch^a into P;
14 **end while**
15 $Ch_{best} \leftarrow \emptyset$;
16 **while** algorithm has not iterated complete **do**
17 calculate fitness value for all $Ch^a \in P$;
18 $Ch_{best} \leftarrow$ the fittest Ch^a;
19 evolve P for chromosome selection, gene crossover and gene mutation;
20 **end while**
21 $Q_{sc} \leftarrow Ch_{best}$;

IOGA is the same as that in ILP model, so the fitness value of chromosome can be calculated by Eq. (2) as well. The fitness value is calculated in every generation to find better chromosomes among population, where the larger fitness value represents a better HC-RMLSA scheme. Chromosome selection is designed as Roulette Wheel Selection [34] in which each chromosome is assigned to a segment based on its fitness value and the virtual roulette wheel is span to pick out chromosomes until the desired number of chromosomes is selected. In the selected chromosomes, multipoint gene crossover is applied for random selecting gene pairs to generate offspring. Fig. 2 (b) illustrates the process of gene crossover (note that we only show a pair of genes as an example), where routing light-path pairs or light-tree pairs are swapped. After gene crossover, gene mutation occurs randomly in the selected chromosomes to keep the diversity of population. The bottom half of Fig. 2 (b) shows the procedure of gene mutation thoroughly, in which mutation also occurs on routing light-path/light-tree of a gene. Moreover, the modulation level and allocated FS's will be recalculated in new genes after gene crossover and mutation if the original one cannot match the new routing light-path/light-tree.

Complexity Analysis: in Algorithm 1, we can pre-calculate three candidate light-paths and light-trees for each possible request when the network topology is determined.

Thus, the time complexity of gene encoding is $O(|I| \cdot |P|)$, and the time complexity of chromosome processing is

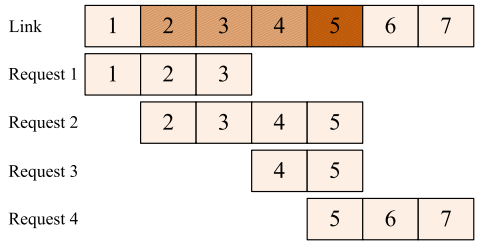

FIGURE 3. FS occupation of a link by holding four requests.

$O(U \cdot |P|)$ with the worst iteration case of algorithm is U. The time complexity of Algorithm 1 is $O(|I| \cdot |P| + U \cdot |P|)$, which is capable in the provisioning of IDC-EONs [23].

B. PRIORITY BASED RATIONALITY ADAPTION

As the SC may occur in HC-RMLSA scheme solved by IOGA, the priority based rationality adaption (PRA) is proposed to eliminate SC. Generally, the set of arriving HCRs and the links with SC in HC-RMLSA scheme are ordered by the corresponding priority principle initially. Then we adjust the location of non-fixed FS's of HCRs to eliminate SC in links. The detailed processes of PRA are demonstrated in two phases in Algorithm 2.

In phase I of Algorithm 2, two priority principles are introduced, and then we describe the sort rules.

Request Priority Principle: We order two HCRs with different actual types according to PPM. User-to-DC traffic is mainly focused when PPM is 2:1, so that the HCR with PTP transmission has a higher priority than that of PTM transmission. DC-to-DC traffic becomes more important when PPM is 1:2, thus, the contrary on the request priority.

When PPM is 1:1, we order the requests randomly. Moreover, two HCRs with the same actual type are ordered by their capacities, in which a larger capacity leads to a higher priority. If the capacities of two HCRs are the same, their order is randomly assigned.

SC Link Priority Principle: There are two definitions for SC links in HC-RMLSA scheme in this paper. 1) Spectrum depth (SD): the maximum occupied number of a FS with SC in the link. 2) Spectrum span (SS): the number of SC FS's in the link.

We first order SC links by their SDs, in which the larger SD leads to higher priority. When two links have the same SD, we order them by SS. The larger SS causes the higher priority. As an example shown in Fig. 3, we assume a fiber link with seven FS's which are used to hold four requests. The occupied FS's of each request is shown in the shallower yellow. The occupied time of each FS in this link is 1, 2, 2, 2, 3, 1, 1, corresponding to the first to seventh FS. Thus, SD of the link is 3 and SS is 4.

In SC elimination phase (Algorithm 2, Phase II), the HC-RMLSA solution of HCR with the highest priority is firstly fixed and the occupation states of fixed FS's are updated. Then the non-fixed SC elimination starts from the ordered links with non-fixed SC by adjusting locations of the SC FS's away from the fixed FS's. The non-fixed FS's adjustment depends on the priority of their corresponding HCRs. Notably, if the non-fixed FS's of a HCR can eliminate SC with the fixed occupied FS's by changing its FS's location, the HC-RMLSA solution can be fixed after the changes; if not, the HCR is blocked. In Fig. 4, we show an example of SC elimination between two HCRs, in which HCR 1 has higher priority than HCR 2. The information of two requests is shown in Fig. 4 (b). The routing light-tree of HCR 1 goes through Links 2-6, 2-3 and 3-4 with the non-fixed FS indexes of 1, 2, and 3. The routing light-path of HCR2 goes through Links 3-4 and 4-5 with the non-fixed FS indexes

Algorithm 2 PRA

Input: G(V, E), Q_{sc}.
Output: HC-RMLSA scheme without SC, Q_{usc}.
Phase I: Sorting HCRs and SC links
check fixed FS's occupation state;
order all requests by *Request Priority Principle*;
SC link set $E_{sc} \leftarrow \emptyset$;
for link $e \in E$ **do**
  if there is SC in the link e **then**
    put link e into E_{sc};
    calculate the values of SD and SS for link e;
  end for
  order each link $e \in E_{sc}$ by *SC Link Priority Principle*;
Phase II: Eliminating SC
fix the HC-RMLSA solution where the corresponding HCR has the highest request priority;
update network state;
put the HC-RMLSA solution where the corresponding HCR has the highest request priority into Q_{usc} and remove it from Q_{sc};
for each ordered link $e \in E_{sc}$ **do**
  for each ordered HCR $i \in I$ **do**
    if assigned FS's of HCR i cause SC in link e **then**
      adjust the assigned FS's index to eliminate SC with fixed FS's in network;
      if adjustment succeed **then**
        fix the adjusted HC-RMLSA solution;
        update fixed FS's occupation state;
        put the adjusted HC-RMLSA solution into Q_{usc} and remove the old one from Q_{sc};
      else HCR i is blocked;
    end for
end for

TABLE 1. Parameter values of IOGA-PRA.

Crossover rate	0.9
Mutation rate	0.2
# of chromosomes	50
# of generations	60

TABLE 2. σ-values of different algorithms in 6-node network under static network scenario.

# of HCR	LIP			IOGA-PRA			HC-RMLSA-GA		
	1:2	2:1	1:1	1:2	2:1	1:1	1:2	2:1	1:1
5	26.3	25.1	25.8	22.5	18.7	20.1	19.6	14.2	17.5
10	207.7	184.7	204.2	194.4	179.7	186.5	183.4	166.7	176.1

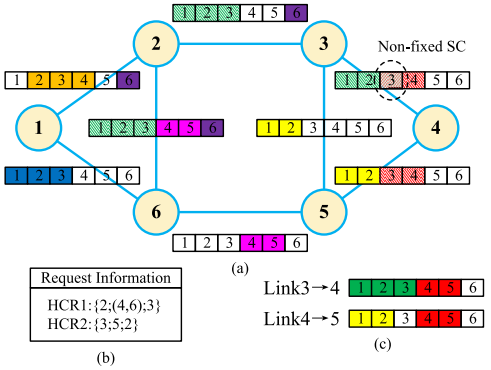

FIGURE 4. An example of SC elimination in six-node network topology where (a) state of current network FS occupation and non-fixed FS's, (b) HCR information, and (c) state of FS occupation in Link 3-4 and 4-5 after SC elimination.

of 3 and 4. The SC occurs on the third FS of Link 3-4 as shown in Fig. 4(a). Due to the higher request priority, the allocated FS's of HCR 1 are fixed at first and the FS location of HCR 2 is adjusted. Fig. 4(c) indicates the new FS locations of HCR 2 after successful adjustment.

Complexity analysis: in Algorithm 2, the time complexity of Phase I and Phase II are $O(|E|)$ and $O(|E| \cdot |I|)$, respectively. Thus, the time complexity of Algorithm 2 is $O(|E| + |E| \cdot |I|)$, which is capable in the provisioning of IDC-EONs [23].

VI. PERFORMANCE EVALUATION

In this section, numerical results of HC-RMLSA with global optimization in network performance under both static and dynamic network scenarios are presented. We measure the algorithm efficiency of proposed IOGA-PRA by comparing it with the formulated ILP model in small-scale network topology under static network scenario. Moreover, the algorithm performance of IOGA-PRA is evaluated by comparing it to other four benchmark algorithms with different objectives under large-scale network topology in both static and dynamic scenarios.

To evaluate network performance in σ, spectrum utilization and NEC, we implement four benchmark algorithms with the above objectives. A pure GA based HC-RMLSA algorithm (HC-RMLSA-GA) referred from [35] is implemented with the objective of optimizing σ. A HC-RMLSA with layered minimum spanning tree (HC-RMLSA-LMST) based on the proposed algorithm in [36], is implemented to improve network spectrum utilization. To achieve efficient NEC, pure energy-efficient HC-RMLSA algorithm (PEEM-HC-RMLSA) and blocking aware-EEM HC-RMLSA algorithm (BAEEM-HC-RMLSA) are implemented based on the algorithms proposed in [5].

TABLE 3. Average running time of different algorithms in 6-node network under static network scenario in seconds.

HCR #	LIP	IOGA-PRA	HC-RMLSA-GA
5	1982	0.4661	0.2125
10	7553	0.7537	0.6039

A. STATIC IDC-EON PLANNING

In this section, we evaluate the ILP model, IOGA-PRA, and benchmark algorithms under static network scenario, in which all HCRs are known ahead of time. Two test network topologies, i.e., 6-node network and 14-node NSFNET [11], are used for static scenario. The actual types of HCR are defined as anycast, unicast, multicast and manycast randomly. When actual type is anycast, HCR is defined as three candidate destination nodes, of which one should be reached; when actual type is multicast, HCR is defined as three destination nodes; and when actual type is manycast, HCR is defined as three candidate destination nodes, of which two should be reached. The source node, destination node(s) and candidate destination nodes are randomly selected in network nodes without repetition among them of each HCR. In addition, the capacity of each HCR is allocated within the range [10-100] Gbit/s @1Gbit/s granularity.

The ILP model is solved by IBM ILOG CPLEX optimizer [37], meanwhile, the heuristic algorithms are simulated by C++ programming directly. All simulations are completed on a computer with 4.00 GB RAM, i5-4590 CPU and 3.30GHz Inter Core. Table 1 shows the main parameter setting of IOGA-PRA. To decrease the average running time of ILP model, we only consider 50 FS's in each fiber link of 6-node network, where bandwidth of each FS is 12.5 GHz. However, in NSFNET, we assume that the network is at C waveband which means there is almost 4.45THz spectrum resource on each optical fiber, i.e., about 356 FS's in each fiber link with 12.5 GHz granularity.

Table 2 shows the values of σ with five and ten arriving HCRs under 6-node network topology, in which the proposed IOGA-PRA performs closely to the solutions solved by ILP model in different PPMs. It is demonstrated that the high efficiency of IOGA-PRA in improving overall network performance by efficient processing a set of HCRs and rational adapting of SC links. The average running times of algorithms are shown in Table 3. The ''average'' here has two senses, i.e., the average running time under different

TABLE 4. σ-values of different algorithms in NSFNET under static network scenario with PPM equals to 1:2.

# of HCR	IOGA -PRA	HC-RMLSA-GA	HC-RMLSA-LMST	PEEM-HC-RMLSA	BAEEM-HC-RMLSA
5	0.063	0.058	0.054	0.054	0.057
10	0.217	0.194	0.161	0.147	0.154
30	1.425	1.366	1.183	1.253	1.186
50	2.759	2.513	2.309	2.376	2.308
100	6.634	6.279	5.517	5.961	5.764

*All σ -values should be multiplied 10^4 with the unit of Gbit·km/J.

TABLE 5. σ-values of different algorithms in NSFNET under static network scenario with PPM equals to 2:1.

# of HCR	IOGA -PRA	HC-RMLSA-GA	HC-RMLSA-LMST	PEEM-HC-RMLSA	BAEEM-HC-RMLSA
5	0.049	0.042	0.040	0.036	0.038
10	0.145	0.135	0.113	0.085	0.092
30	1.073	0.987	0.871	0.883	0.832
50	1.855	1.743	1.726	1.799	1.755
100	6.047	5.628	5.562	5.583	5.306

*All σ -values should be multiplied 10^4 with the unit of Gb·km/J.

TABLE 6. σ-values of different algorithms in NSFNET under static network scenario with PPM equals to 1:1.

# of HCR	IOGA -PRA	HC-RMLSA-GA	HC-RMLSA-LMST	PEEM-HC-RMLSA	BAEEM-HC-RMLSA
5	0.054	0.046	0.043	0.039	0.044
10	0.168	0.153	0.125	0.116	0.113
30	1.294	1.210	1.037	1.095	1.132
50	2.147	2.075	1.652	1.799	1.678
100	6.281	6.011	5.477	5.734	5.534

*All σ -values should be multiplied 10^4 with the unit of Gbit·km/J.

TABLE 7. The maximum used FS index of different algorithms in NSFNET under static network scenario with PPM equals to 1:2.

# of HCR	IOGA -PRA	HC-RMLSA-GA	HC-RMLSA-LMST	PEEM-HC-RMLSA	BAEEM-HC-RMLSA
5	7.6	7.9	6.2	8.0	7.9
10	20.3	23.4	9.2	12.6	11.8
30	26.7	29.3	21.3	30.9	28.9
50	32.5	37.3	42.8	49.3	47.5
100	50.9	56.6	71.7	81.4	77.3

PPMs and the average running time with the repeated running of algorithms. We observe that IOGA-PRA is much more efficient than ILP model due to the less algorithm complexity. However, the running time of HC-RMLSA-GA is less than that of IOGA-PRA. This is because HC-RMLSA-GA only encodes one request each time to form a population and without rationality adaption, whereas IOGA-PRA encodes all arriving requests to form a large-scale population and rationality adaption operation which increases algorithm complexity.

To further evaluate algorithm performance, we simulate IOGA-PRA and four benchmark algorithms in NSFNET. The simulation results of σ-value are shown in Tables 4, 5, and 6 which depicts that IOGA-PRA can provide better σ-values under different PPMs and request numbers. The improvement in σ-value of IOGA-PRA is about 4.3%-47.6%, 7.4%-65.6%, and 3.5%-48.7% compared with other four benchmark algorithms under PPM of 1:2, 2:1, and 1:1, respectively.

To estimate the effect of optimizing overall network performance to main network metrics (i.e., network spectrum utilization and NEC) in static scenario, we analyze the maximum used FS index and NEC with different numbers of requests and PPMs. Tables 7, 8, and 9 show the results of the maximum used FS index. We observe that the results provided by IOGA-PRA are worse than that solved by HC-RMLSA-LMST when HCR number is no more than 30. This is because IOGA-PRA balances network spectrum utilization and NEC to reach a co-suboptimum result during the overall network performance improvement, which leads to a worse result in the maximum used FS index. Moreover, the network available spectrum resource decreases with increasing request numbers, thus, the cooperation of all arriving HCRs of IOGA-PRA results in a better network spectrum utilization when the number of HCRs is increasing. Table 10, 11, and 12 show the results of NEC under different PPMs and request numbers, in which the results of

TABLE 8. The maximum used FS index of different algorithms in NSFNET under static network scenario with PPM equals to 2:1.

# of HCR	IOGA -PRA	HC-RMLSA- GA	HC-RMLSA- LMST	PEEM-HC- RMLSA	BAEEM-HC- RMLSA
5	8.3	8.9	7.1	8.9	8.7
10	25.4	27.6	12.3	14.7	13.9
30	29.8	33.3	27.4	35.2	34.9
50	37.2	40.9	48.3	59.1	57.5
100	56.7	61.8	82.9	97.5	94.7

TABLE 9. The maximum used FS index of different algorithms in NSFNET under static network scenario with PPM equals to 1:1.

# of HCR	IOGA- PRA	HC-RMLSA- GA	HC-RMLSA- LMST	PEEM-HC- RMLSA	BAEEM-HC- RMLSA
5	8.0	8.4	6.7	8.5	8.1
10	24.6	26.3	10.4	13.5	12.7
30	28.5	31.8	24.7	32.1	30.3
50	35.9	38.7	45.5	52.7	51.6
100	52.1	59.4	76.2	84.8	80.5

TABLE 10. NEC of different algorithms in NSFNET under static network scenario with PPM equals to 1:2.

# of HCR	IOGA -PRA	HC- RMLSA-GA	HC-RMLSA- LMST	PEEM-HC- RMLSA	BAEEM-HC- RMLSA
5	0.065	0.070	0.075	0.078	0.082
10	0.076	0.079	0.082	0.090	0.095
30	0.113	0.117	0.123	0.119	0.124
50	0.147	0.155	0.162	0.154	0.162
100	0.243	0.251	0.268	0.249	0.268

*All values of NEC should be multiplied 10^5 with the unit of W.

TABLE 11. NEC of different algorithms in NSFNET under static network scenario with PPM equals to 2:1.

# of HCR	IOGA -PRA	HC- RMLSA-GA	HC-RMLSA- LMST	PEEM-HC- RMLSA	BAEEM-HC- RMLSA
5	0.085	0.092	0.114	0.109	0.112
10	0.107	0.114	0.132	0.120	0.125
30	0.145	0.152	0.168	0.151	0.159
50	0.172	0.178	0.212	0.183	0.192
100	0.311	0.319	0.347	0.314	0.329

*All values of NEC should be multiplied 10^5 with the unit of W.

TABLE 12. NEC of different algorithms in NSFNET under static network scenario with PPM equals to 1:1.

# of HCR	IOGA -PRA	HC- RMLSA-GA	HC-RMLSA- LMST	PEEM-HC- RMLSA	BAEEM-HC- RMLSA
5	0.078	0.081	0.105	0.098	0.105
10	0.085	0.089	0.117	0.109	0.117
30	0.129	0.134	0.153	0.140	0.149
50	0.161	0.167	0.197	0.172	0.183
100	0.269	0.280	0.323	0.288	0.315

*All values of NEC should be multiplied 10^5 with the unit of W.

IOGA-PRA are always kept at a minimum. This is due to NEC, as network cost, is considered in the optimization goal of IOGA-PRA, so that IOGA-PRA can dedicate to energy saving. From all the results in static scenario, the different values of PPM are influenced on the specific numerical values of results while the trends of results keep the same.

B. DYNAMIC IDC-EON PROVISIONING

In this section, algorithms are simulated with dynamic HCRs, i.e., HCR is time-variable which can arrive and leave during network operation, in NSFNET. We assume that HCRs are formed as a Poisson process with average arrival rate λ and the service time of each HCR has formed an exponential distribution with mean value μ. The traffic load is denoted

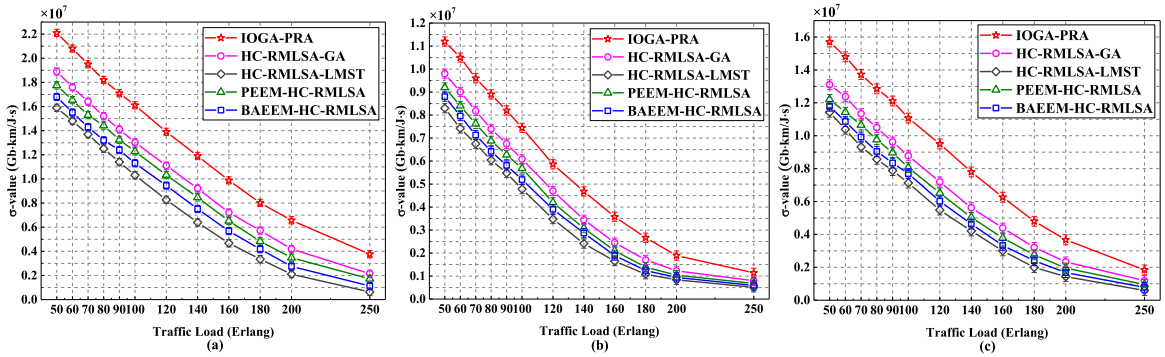

FIGURE 5. σ **-values in NSFNET under PPM of (a) 2:1, (b) 1:2, and (c) 1:1.**

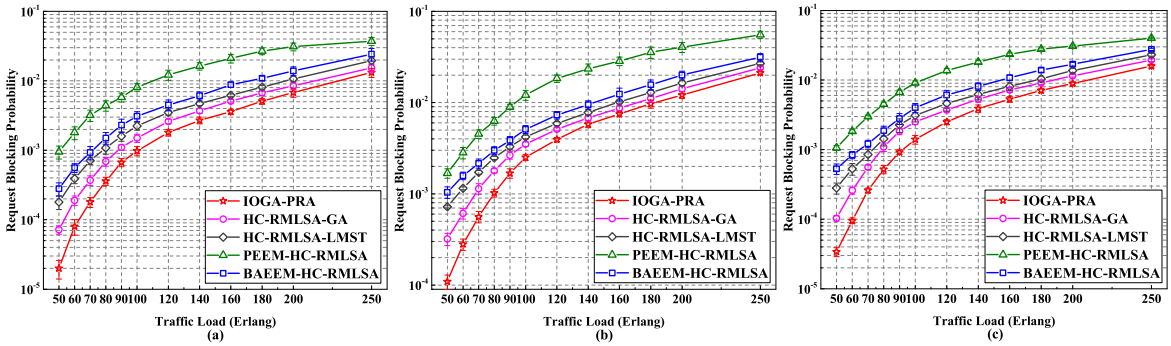

FIGURE 6. **RBP in NSFNET under PPM of (a) 2:1, (b) 1:2, and (c) 1:1.**

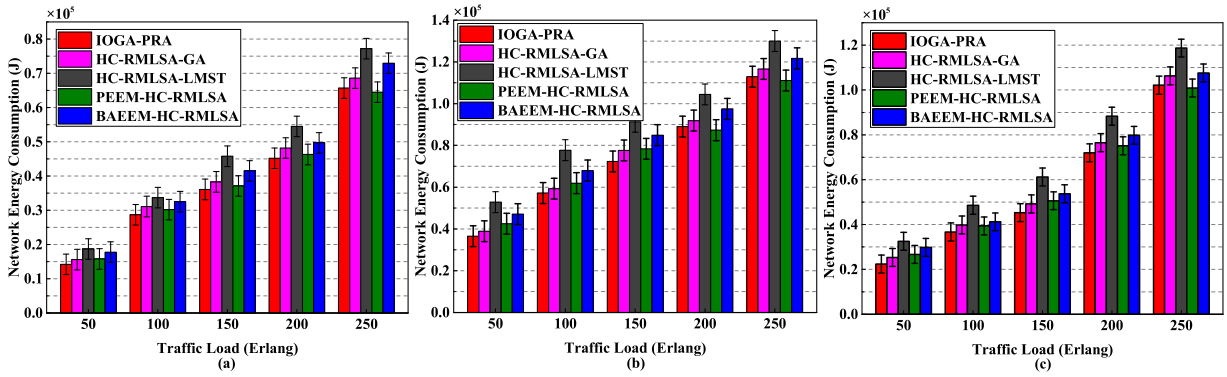

FIGURE 7. **NEC in NSFNET under PPM of (a) 2:1, (b) 1:2, and (c) 1:1.**

as λ/μ in Erlang, which varies within [50-250] Erlang by setting $1/\mu = 5$ and changing λ from 10 to 50. The number of HCRs that is processed by IOGA-PRA each time is set as 10. Other simulation parameters are the same as that in static scenario. All results are computed over multiple simulations to achieve 95% confidence interval.

In Fig. 5 (a), (b), and (c), the σ-values of algorithms are depicted in different PPMs. We observe that IOGA-PRA can always provide a better σ-values in different traffic loads and PPMs, with the improvement of 23.7%-86.2%, 12.0%-77.2%, and 12.5%-80.3% in PPM equivalent to 2:1, 1:2 and 1:1, respectively. This is due to the fact that IOGA-PRA operates a set of HCRs simultaneously to reach better HC-RMLSA solutions by SC toleration, and the PRA coordinates these HC-RMLSA solutions to satisfy their feasibility.

To estimate the effect of optimizing overall network performance to main network metrics in dynamic scenario, we simulate the values of RBP and NEC of algorithms in different traffic loads and PPMs that are shown in Fig. 6 and Fig. 7. It is obvious that the RBPs of IOGA-PRA keep the minimum under different traffic loads and PPMs in Fig. 6(a), (b), and (c), which reflect the optimization process of IOGA-PRA focuses on the network resource load balance and can further reduce the RBP. The reduction of RBP of IOGA-PRA is about 14.3%-85.6%, 8.9%-76.8%

and 11.6%-80.2% compared with four benchmark algorithms under the PPM of 2:1, 1:2, and 1:1, respectively. In Fig. 7(a), (b), and (c), the NEC of IOGA-PRA becomes higher when traffic loads up to 200 Erlang, while it maintains at a minimum when traffic loads lower than 200 Erlang with all kinds of PPMs. The reason for this variation trend is that IOGA-PRA serves the most number of HCRs compared with benchmark algorithms and the coordination of a set of HCRs becomes harder due to the decrease available spectrum resource with traffic load increase, which further brings about the larger energy consumption in network.

VII. CONCLUSION

In this paper, we investigate the global optimization of IDC-EON performance with hybrid-cast traffic. We first define how to evaluate overall network performance by cost-effectiveness value. Then an ILP model is proposed to formulate the HC-RMLSA problem with the objective of maximizing overall network performance in static network scenario. Furthermore, the IOGA-PRA is proposed to address the efficient HC-RMLSA solutions with outstanding overall network performance by request-independent spectrum assignment and priority based rationality adaption of HC-RMLSA scheme in both static and dynamic network scenarios. Simulation results demonstrate that IOGA-PRA can provide quite good HC-RMLSA solutions, which have slightly disparity with the optimal schemes solved by ILP model in static small-scale network planning. It can also achieve corresponding maximum overall network performance improvement of 47.6%, 65.6% and 48.7% compared with four benchmark algorithms under the PPM of 1:2, 2:1 and 1:1 in NSFNET. As for dynamic network provisioning, the IOGA-PRA can reach the maximum improvement in overall network performance of 86.2%, 77.2% and 80.3% with the minimum RBP maintaining and acceptable NEC increase, compared with four benchmark algorithms under the PPM of 2:1, 1:2 and 1:1, respectively. Although the proposed criterion and IOGA-PRA have been achieved obvious effect in the overall network performance evaluation and the global optimization of network performance respectively, there are still some practical issues to be further investigated. Firstly, with the modularization of network elements, designing and operation of the IDC-EONs gradually changes from the traditional static manner to dynamic adaption, which lead to the variation of CapEx. We will investigate this in our future work and expect that the updated criterion can measure the overall network performance better. Meanwhile, the IDC-EON topology that partial network nodes connecting DCs would be more practical, the influence of the number of DCs to overall network performance will be addressed in our future work as well.

REFERENCES

[1] X. Zhao, V. Vusirikala, B. Koley, V. Kamalov, and T. Hofmeister, "The prospect of inter-data-center optical networks," *IEEE Commun. Mag.*, vol. 51, no. 9, pp. 32–38, Sep. 2013.
[2] A. Muhammad, N. Skorin-Kapov, and L. Wosinska, "Manycast and anycast routing for replica placement in datacenter networks," in *Proc. Eur. Conf. Opt. Commun. (ECOC)*, Valencia, Spain, Sep./Oct. 2015, pp. 1–3.
[3] R. Goścień, K. Walkowiak, and M. Tornatore, "Survivable multipath routing of anycast and unicast traffic in elastic optical networks," *IEEE/OSA J. Opt. Commun. Netw.*, vol. 8, no. 6, pp. 343–355, Jun. 2016.
[4] X. Li, L. Zhang, Y. Tang, J. Guo, and S. Huang, "Distributed sub-tree-based optical multicasting scheme in elastic optical data center networks," *IEEE Access*, vol. 6, pp. 6464–6477, 2018.
[5] A. Fallahpour, H. Beyranvand, and J. A. Salehi, "Energy-efficient manycast routing and spectrum assignment in elastic optical networks for cloud computing environment," *J. Lightw. Technol.*, vol. 33, no. 19, pp. 4008–4018, Oct. 1, 2015.
[6] B. Jennings and R. Stadler, "Resource management in clouds: Survey and research challenges," *J. Netw. Syst. Manage.*, vol. 23, no. 3, pp. 567–619, 2015.
[7] M. Jinno, "Elastic optical networking: Roles and benefits in beyond 100-Gb/s Era," *J. Lightw. Technol.*, vol. 35, no. 6, pp. 1116–1124, Mar. 1, 2017.
[8] Y. Tao *et al.*, "Modulation format independent blind polarization demultiplexing algorithms for elastic optical networks," *Sci. China Inf. Sci.*, vol. 60, p. 022305, Feb. 2017.
[9] M. Zeng, W. Fang, and Z. Zhu, "Orchestrating tree-type VNF forwarding graphs in inter-DC elastic optical networks," *J. Lightw. Technol.*, vol. 34, no. 14, pp. 3330–3341, Jul. 15, 2016.
[10] B. C. Chatterjee, N. Sarma, and E. Oki, "Routing and spectrum allocation in elastic optical networks: A tutorial," *IEEE Commun. Surveys Tuts.*, vol. 17, no. 3, pp. 1776–1800, 3rd Quart., 2015.
[11] H. Chen, Y. Zhao, J. Zhang, W. Wang, and R. Zhu, "Static routing and spectrum assignment for deadline-driven bulk-data transfer in elastic optical networks," *IEEE Access*, vol. 5, pp. 13645–13653, 2017.
[12] L. Zhang and Z. Zhu, "Dynamic anycast in inter-datacenter networks over elastic optical infrastructure," in *Proc. Comput., Netw. Commun. (ICNC)*, Honolulu, HI, USA, Feb. 2014, pp. 491–495.
[13] J. Wu, Z. Ning, and L. Guo, "Energy-efficient survivable grooming in software-defined elastic optical networks," *IEEE Access*, vol. 5, pp. 6454–6463, 2017.
[14] M. Noormohammadpour and C. S. Raghavendra. (2017). "Datacenter traffic control: Understanding techniques and trade-offs." [Online]. Available: https://arxiv.org/abs/1712.03530
[15] M. F. Habib, M. Tornatore, M. D. Leenheer, F. Dikbiyik, and B. Mukherjee, "Design of disaster-resilient optical datacenter networks," *J. Lightw. Technol.*, vol. 30, no. 16, pp. 2563–2573, Aug. 15, 2012.
[16] A. Muhammad, N. Skorin-Kapov, and M. Furdek, "Manycast, anycast, and replica placement in optical inter-datacenter networks," *IEEE/OSA J. Opt. Commun. Netw.*, vol. 9, no. 12, pp. 1161–1171, Dec. 2017.
[17] R. Lin, M. Zukerman, G. Shen, and W.-D. Zhong, "Design of light-tree based optical inter-datacenter networks," *IEEE/OSA J. Opt. Commun. Netw.*, vol. 5, no. 12, pp. 1443–1455, Dec. 2013.
[18] M. Aibin and K. Walkowiak, "Dynamic routing of anycast and unicast traffic in elastic optical networks with various modulation formats—Trade-off between blocking probability and network cost," in *Proc. HPSR*, Vancouver, BC, Canada, Jul. 2014, pp. 64–69.
[19] L. Zhang and Z. Zhu, "Spectrum-efficient anycast in elastic optical inter-datacenter networks," *Opt. Switching Netw.*, vol. 14, no. 3, pp. 250–259, Aug. 2014.
[20] H. Yang *et al.*, "Global resources integrated resilience for software defined data center interconnection based on IP over elastic optical network," *IEEE Commun. Lett.*, vol. 18, no. 10, pp. 1735–1738, Oct. 2014.
[21] L. Gong, X. Zhou, W. Lu, and Z. Zhu, "A two-population based evolutionary approach for optimizing routing, modulation and spectrum assignments (RMSA) in O-OFDM networks," *IEEE Commun. Lett.*, vol. 16, no. 9, pp. 1520–1523, Sep. 2012.
[22] P. Lechowicz and K. Walkowiak, "Genetic algorithm for routing and spectrum allocation in elastic optical networks," in *Proc. ENIC*, Wroclaw, Poland, Sep. 2016, pp. 273–280.
[23] L. Gong, X. Zhou, X. Liu, W. Zhao, W. Lu, and Z. Zhu, "Efficient resource allocation for all-optical multicasting over spectrum-sliced elastic optical networks," *J. Opt. Commun. Netw.*, vol. 5, no. 8, pp. 836–847, Aug. 2013.
[24] Z. Zhu *et al.*, "Impairment- and splitting-aware cloud-ready multicast provisioning in elastic optical networks," *IEEE/ACM Trans. Netw.*, vol. 25, no. 2, pp. 1220–1234, Apr. 2017.
[25] A. Betker, D. Kosiankowski, C. Lange, F. Pfeuffer, C. Raack, and A. Werner, "Energy efficiency in extensive multilayer core and regional networks with protection," Telecommun., ZIB, Berlin, Germany, ZIB-Rep. 12-45, Dec. 2012. [Online]. Available: https://opus4.kobv.de/opus4-zib/frontdoor/index/index/docId/1715

[26] L. Yang, L. Gong, F. Zhou, B. Cousin, M. Molnár, and Z. Zhu, "Leveraging light forest with rateless network coding to design efficient all-optical multicast schemes for elastic optical networks," *J. Lightw. Technol.*, vol. 33, no. 18, pp. 3945–3955, Sep. 15, 2015.
[27] M. Jinno *et al.*, "Distance-adaptive spectrum resource allocation in spectrum-sliced elastic optical path network," *IEEE Commun. Mag.*, vol. 48, no. 8, pp. 138–145, Aug. 2010.
[28] M. Eiselt, B. T. Teipen, K. Grobe, A. Autenrieth, and J.-P. Elbers, "Programmable modulation for high-capacity networks," in *Proc. Eur. Conf. Opt. Commun. (ECOC)*, Geneva, Switzerland, 2011, pp. 1–3.
[29] M. H. Eiselt, H. Griesser, A. Autenrieth, B. T. Teipen, and J.-P. Elbers, "Programmable modulation for high-capacity networks," in *Proc. OECC*, Busan, South Korea, Jul. 2012, pp. 771–772.
[30] R. Huelsermann, M. Gunkel, C. Meusburger, and D. A. Schupke, "Cost modeling and evaluation of capital expenditures in optical multilayer networks," *J. Opt. Netw.*, vol. 7, no. 9, pp. 814–833, 2008.
[31] P. Papanikolaou *et al.*, "Minimizing energy and cost in fixed-grid and flex-grid networks," *IEEE/OSA J. Opt. Commun. Netw.*, vol. 7, no. 4, pp. 337–351, Apr. 2015.
[32] A. Nag, M. Tornatore, and B. Mukherjee, "Energy-efficient and cost-efficient capacity upgrade in mixed-line-rate optical networks," *IEEE/OSA J. Opt. Commun. Netw.*, vol. 4, no. 12, pp. 1018–1025, Dec. 2012.
[33] J. R. Koza, *Genetic Programming: On the Programming of Computers by Means of Natural Selection*. Cambridge, MA, USA: MIT Press, 1992.
[34] R. Kumar, and Jyotishree, "Blending roulette wheel selection & rank selection in genetic algorithm," *Int. J. Mach. Learn. Comput.*, vol. 2, no. 4, pp. 365–370, 2012.
[35] X. Luo *et al.*, "Manycast routing, modulation level and spectrum assignment over elastic optical networks," *Opt. Fiber Technol.*, vol. 36, pp. 317–326, Jul. 2017.
[36] X. Liu, L. Gong, and Z. Zhu, "Design integrated RSA for multicast in elastic optical networks with a layered approach," in *Proc. GLOBECOM*, Atlanta, GA, USA, Dec. 2013, pp. 2346–2351.
[37] International Business Machines Corp. *IBM ILOG CPLEX Optimizer12.3*. Accessed: Aug. 6, 2012. [Online]. Available: http://www.01.ibm.com/software/integration/optimization/cplex-optimizer/

XIAO LUO received the B.S. degree from the Beijing University of Posts and Telecommunications in 2014, where she is currently pursuing the Ph.D. degree in electronic science and technology. Her research interests include routing, modulation-level and spectrum assignment strategy in elastic optical networks, and optical network survivability.

CHEN SHI received the B.S. degree from the Beijing University of Posts and Telecommunications, Beijing, China, and the M.S. degree from the University of Florida, Gainesville, FL, USA. She is currently pursuing the Ph.D. degree with Iowa State University, Ames, IA, USA. Her main research interests focus on computer network and Android platform.

XUE CHEN received the B.S. degree from the Dalian University of Technology, Dalian, China, in 1982, and the M.S. degree from the Beijing University of Posts and Telecommunications (BUPT), Beijing, China, in 1985. She is currently a Professor with the Institute of Information Photonics and Optical Communications, BUPT. Her main research interests focus on backbone optical transmission and optical access networks.

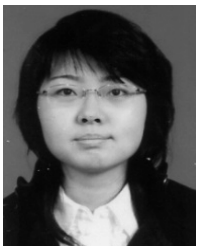

LIQIAN WANG received the B.S. and Ph.D. degrees from the Beijing University of Posts and Telecommunications (BUPT), Beijing, China, in 2003 and 2010, respectively. Since 2010, she has been a Lecturer with the Institute of Information Photonics and Optical Communications, BUPT. Her research interests include FEC and modulation technologies for backbone optical transmission and optical access networks.

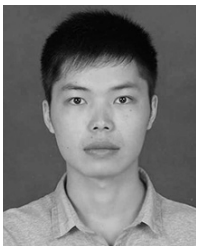

TAO YANG received the B.S. degree from the Southwest University of Science and Technology, China, in 2014. He is currently pursuing the Ph.D. degree in information and communication engineering with the Beijing University of Posts and Telecommunications, Beijing, China. His research interests focus on high-speed coherent optical transmission and digital signal processing algorithm in elastic optical networks.